Metabolomics (2024) 20:55
https://doi.org/10.1007/s11306-024-02121-2

ORIGINAL ARTICLE

Analysis of the metabolic profile of humans naturally exposed to RF-EM radiation

Neel Mani Rangesh[1] · Arun Kumar Malaisamy[2] · Nitesh Kumar[3] · Sanjay Kumar[1]

Received: 28 September 2023 / Accepted: 20 April 2024 / Published online: 18 May 2024
© The Author(s), under exclusive licence to Springer Science+Business Media, LLC, part of Springer Nature 2024

Abstract

Introduction The world is experiencing exponential growth in communication, especially wireless communication. Wireless connectivity has recently become a part of everyone's daily life. Recent developments in low-cost, low-power, and miniature devices contribute to a significant rise in radiofrequency-electromagnetic field (RF-EM) radiation exposure in our environment, raising concern over its effect on biological systems. The inconsistent and conflicting research results make it difficult to draw definite conclusions about how RF-EM radiation affects living things.

Objectives This study identified two micro-environments based on their level of exposure to cellular RF-EM radiation, one with significantly less exposure and another with very high exposure to RF-EM radiation. Emphasis is given to studying the metabolites in the urine samples of humans naturally exposed to these two different microenvironments to understand short-term metabolic dysregulations.

Methods Untargeted ^{1}H NMR spectroscopy was employed for metabolomics analyses to identify dysregulated metabolites. A total of 60 subjects were recruited with 5 ml urine samples each. These subjects were divided into two groups: one highly exposed to RF-EM ($n = 30$) and the other consisting of low-exposure populations ($n = 30$).

Results The study found that the twenty-nine metabolites were dysregulated. Among them, 19 were downregulated, and 10 were upregulated. In particular, Glyoxylate and dicarboxylate and the TCA cycle metabolism pathway have been perturbed. The dysregulated metabolites were validated using the ROC curve analysis.

Conclusion Untargeted urine metabolomics was conducted to identify dysregulated metabolites linked to RF-EM radiation exposure. Preliminary findings suggest a connection between oxidative stress and gut microbiota imbalance. However, further research is needed to validate these biomarkers and understand the effects of RF-EM radiation on human health. Further research is needed with a diverse population.

Keywords Radiofrequency-electromagnetic field (RF-EM) radiation · Human urine · Untargeted metabolomics · NMR spectroscopy · Oxidative metabolism

1 Introduction

The increasing use of technology such as Low Power Wide Area Networks (LPWA) and Wireless Body Area Networks (WBAN) has led to the development of wireless communication that can be used in many different areas of life, including consumer electronics, healthcare, communication, banking, and more RFID (Radio Frequency Identifiers) microchips are now available for sizes as small as a grain of rice and can be implanted in humans, animals, and plants or attached to anything or any possessions. In an alarming evaluation, the International Agency for Research on Cancer (IARC) has said that "Radiofrequency electromagnetic fields are possibly carcinogenic to humans (Group 2B)" (2013). As

✉ Neel Mani Rangesh
neelmr@gmail.com

[1] Department of Electronics & Communication Engineering, Birla Institute of Technology, Mesra, Ranchi, Jharkhand 835 215, India

[2] Transcription Regulation Group, International Centre for Genetic Engineering and Biotechnology (ICGEB), Aruna Asaf Ali Marg, New Delhi 110 067, India

[3] Department of Pathology, Indira Gandhi Institute of Medical Sciences (IGIMS), Sheikhpura, Patna, Bihar 800 014, India

Table 1 EMF power density measured through field strength analyzer for microenvironment with (A) less exposure and (B) high exposure to RF-EM radiation

Microenvironment	Latitude	Longitude	Max power density	Average power density
A	27.42105	84.09764	46.50 $\mu W/m^2$	45.17 $\mu W/m^2$
B	25.60841	85.13806	153.2 mW/m^2	126.8 mW/m^2

the use of wireless technology expands, there is a growing interest in studying the potential biological effects of RF-EM radiation, especially in the context of future wireless technology that uses Millimeter waves. Researchers are looking at ways to measure the impact of this radiation, particularly in terms of its potential to cause heating or thermal effects on living organisms (Wood et al., 2017; Lv & Liu, 2003; Wang et al., 2016). However, proof of the non-thermal impacts is not convincing, and many studies investigating non-thermal effects continue.

Some epidemiological examinations have observed a relationship between frequent mobile phone usage and severe diseases such as cancer (Gong et al., 2017; Siddiqi & Al Nazwani, 2019; Habauzit et al., 2014). Dysregulation in metabolic pathways is one of the early manifestations of any disease condition. Thus, we need to study and identify the changes in the metabolic profile of humans naturally exposed to different levels of RF-EM radiations and to find changes in metabolic pathways (Wyde et al., 2016; Robert et al., 2011; Lin, 2019; Danker-Hopfe et al., 2020). The systematic study of the chemical products or metabolites that cells and humans produce is the focus of the relatively new field of "omics" science known as metabolomics. The metabolome, or the total number of metabolites in an organism, can be a particularly sensitive indicator of an organism's phenotype since metabolites are the by-products of several genomes- or proteome-wide interactions. The correlation between dysregulated metabolites in populations with high-radiation exposure, if any, and RF-EM radiation will likely provide much insight into understanding short-term metabolic dysregulations. It will also provide an accurate and deep understanding of the adequacy of current limits of RF-EM radiation standards. This study aimed to identify changes in the metabolomic profile of people naturally exposed to high levels of RF-EM radiation compared to a healthy group of people. We wanted to see if there is a correlation between exposure to RF-EM radiation and changes in metabolic signatures and identify the metabolic pathways affected by this exposure. We used a metabolomics approach to differentiate between the two groups and track changes in catabolic and oxidative metabolites over time following exposure to RF-EM radiation.

2 Methodology

2.1 Subjects recruitment

The prospective urine metabolomics study investigated the metabolic dysregulation of RF-exposed and less-exposed human subjects. The urine samples were collected after the approval from the Institute Ethical Committees (IEC) of Indira Gandhi Institute of Medical Sciences (IGIMS), Patna (1145/IEC/IGIMS/2019/16.10.2019). Written and signed informed consent were sought and obtained from all participants. Before obtaining consent, the Patient's Information Sheet (PIS) and Patient's Informed Consent Form (PICF) were explained to the patients and attendants in multilingual English and Hindi. Thirty healthy subjects highly exposed to RF-EM radiation were recruited from the microenvironment—Marwari Awas Compound, Fraser Road, Patna 800 001 Bihar India (25.60841 N, 85.13806 E). The location was selected through a NARDA-brand Field Strength Analyzer survey for a high EM power density location with an average power density of 126.8 mW/m^2 (Table 1). However, the thirty age-matched healthy individuals with no record of exposure to RF-EMF radiation exposure or a significantly lesser extent were recruited as a comparison group from the microenvironment (Table 2). Similarly, the location of this subject was selected through Village Kamarchinva Done, PO Naurangia, Ramnagar Block, District: West Champaran 845 106, Bihar India (27.42105 N, 84.09764 E) selected

Table 2 Distribution of age profile of subjects highly exposed and less exposed to RF-EM radiation*

Age-group	Less exposure (A)	High exposure (B)
19–25	5	7
26–35	6	7
36–45	10	12
46–55	8	3
56–58	1	1
Total	30	30

*Individuals are residents of the microenvironments and therefore exposed continuously to field strength of the microenvironment

through survey from NARDA-brand Field Strength Analyzer for significantly less EM power density location with average power density of 45.17 μW/m^2 (Table 1). All subjects were male and above 19 years old. The subjects were recruited during the study period of November 2019 to July 2022.

Subjects were randomly and independently recruited at two different RF-EM radiation-exposed microenvironments. 30 clinically healthy males naturally exposed to RF-EM radiation, i.e., spending at least 12 h of daily routine in 500 m proximity to RF-EM radiation source, and 30 age-matched healthy individuals who were not exposed/less exposed to RF-EMF radiation for three years were recruited. All the subjects were recruited after consent was obtained to participate in the study.

Selection of all the 60 subjects was made with some exclusion for the following reasons: (i) receiving medication and surgical operation, (ii) suffering from any chronic disease such as diabetes, hypertension, or any other disease that may affect participation in the study. (iii) anyone who is using any form of narcotics like alcohol, tobacco, etc., currently or in the last 10 years; (iv) currently suffering any infectious disease like influenza, typhoid, etc. (v) suffering from diseases like dengue, tuberculosis, malaria, chikungunya, COVID-19, currently or in the last one year, (vi) has changed his residence in last five years and (vii) refused to participate in the study.

2.2 Sample collection

About 5 ml of First Morning Urine (FMU) samples were collected in the morning between 08:00 and 11:00 h after throwing the initial 50 ml (collected once). Subjects were instructed not to eat, smoke, or brush their teeth before sampling. Collected samples were immediately transported to the laboratory in sealed dry ice bags and stored at − 80 °C for Nuclear Magnetic Resonance (NMR) measurement. The urine samples were thawed during NMR analysis, and 0.5 ml of urine samples were transferred in the 1.5 ml Eppendorf tube to centrifuged in 10000×*g* at 4 °C for 10 min to remove solid debris. In addition, 180 μl of supernatant were collected and mixed with 20 μl of 0.15 M potassium phosphate buffer (Composition: 1.5 M KH_2PO_4, 2 mM NaN_3, 4,4-dimethyl-4-silapentane-1-sulfonic acid (DSS), 10% D_2O pH 7.4) and further transferred to 3 mm NMR tubes for measurement. We have used urine for metabolomics as it has no homeostasis mechanism (Fan & Lane, 2016), has the best tolerance for various "changes," and is the most likely place to find early biomarkers of disease (Beckonert et al., 2007; Nicholson & Wilson, 2003; Bollard et al., 2005).

2.3 NMR spectroscopy

In this study, liquid-state ^{1}H NMR spectroscopy was used for the metabolomics analyses. A typical ^{1}H NMR spectrum of urine contains both low and high molecular weight components, which give a broad range of signal line widths: broadbands from protein and lipoprotein signals contribute strongly to the ^{1}H NMR spectra, with sharp peaks from small molecules superimposed on them. The water signal was suppressed using a typical one-dimensional water pre-saturation pulse sequence Nuclear Overhauser Effect Spectroscopy Gradient-enhanced Purge and Pre-saturation One-Dimensional (NOESYGPPR1D). After adjusting the temperature of the sample, several NMR experiments were performed to study the properties of the sample. The experiments included a 1D ^{1}H NOESY presat, a one-dimensional NMR experiment that uses a pre-saturation pulse sequence to suppress the signal from water molecules and obtain information about the spatial proximity of different nuclei in the sample. In addition, two-dimensional (2D) NMR experiments were performed, including a 2D ^{1}H J-resolved experiment, which provides information about the chemical shift and coupling constants in the sample, and a 2D [^{1}H,^{1}H] Total Correlation Spectroscopy (TOCSY) experiment, which correlates signals from protons that are connected through chemical bonds, allowing the determination of through-bond connectivity in the sample.

Sixty samples were measured using a 500 MHz *Neo* NMR spectrometer equipped with a cryogenic 5 mm Triple Resonance Cryogenic Inverse probe head using 10% D_2O at 298 K temperature. Automatic matching, tuning, and shimming of each data were done. 1D ^{1}H spectra were measured using 1D gradient-enhanced NOESY with 64 scans with a relaxation delay of 4 s. The NMR spectral data was collected as Free Induction Decay (FIDs) with a spectral width of 10,417 Hz and an acquisition time of 3.2 s.

2.4 NMR data processing and metabolite identification

All NMR spectra were processed, analyzed, and manually picked using the software package Topspin 4.1.4. The spectra were Fourier transformed after zero-filling to varying points and applying a line-broadening factor of 0.30 Hz. The spectra were manually corrected for phase and baseline; then, the individual peaks were picked manually using the software package. Peaks for each sample were picked and exported to a comma-separated value (CSV) file (González-Domínguez et al., 2020). The creatinine peak intensity was used as a reference for normalizing all other metabolites in the samples. The ppm regions of 0–0.8 (DSS) and 4.5 -5 (water resonance) were deleted from the files using Python 3 (ipykernel) (Jupyter notebook). NMR peak list and intensity

data (Grouped and compiled as ZIP files) were imported into Metaboanalyst 5.0 (a web-based platform for metabolomic data analysis, interpretation, and visualization) for further statistical and pathway analysis. The HMDB database, chenomx evaluation software, and published literature were also used to identify the metabolites.

2.5 Statistical analysis and data validation

Metaboanalyst 5.0 was used for the univariate and multivariate analysis, a web-based server tool comprising several statistical and pathway analysis links with the Kyoto Encyclopedia of Genes and Genomes (KEGG) pathway. The pre-processed, normalized metabolite concentration data were analyzed using the student's *t*-test, fold change, and volcano plot to determine which metabolites were differentially regulated between the high radiation exposure and less exposed groups. The significance cut-off was kept at 0.05 as the p-value and False Discovery Rate (FDR) values so that no more than 5% of the positive results are expected to be false positives.

The normalized data were subjected to distinguish unsupervised and supervised multivariate analysis, including principal component analysis (PCA), and partial least squares-discriminant analysis (PLS-DA) was done to develop a reliable and robust model for identifying and unraveling differential peaks responsible for the separation between and within the cohort, to check for significant changes, using the fold change and the student's *t*-test. PCA describes the variable X without taking into account the data collection Y. The data was acclimatized into fewer variables, which were given scores based on the average weightage of the original variables. Loadings are a profile of that weightage. The preliminary assessment of systematic variation, similarity, and intrinsic groupings between the metabolic data of high-radiation and less-radiation groups was done using PCA. Furthermore, the weighted sum of PLS regression coefficients was calculated to identify significant buckets that contributed most significantly to cluster separation in PLS-DA and were assigned the appropriate metabolite. The collective data was normalized with median, log-transformed, and autoscaling modes applied.

3 Results and discussion

All the samples were measured, and overall, each peak was selected. The statistical tests from both groups revealed significant differences in the relative concentration of metabolites.

3.1 Univariate analysis

We observed 29 such metabolites, with 10 metabolites upregulated and 19 metabolites downregulated in the high-radiation population. HRE represents a high-radiation exposed population, and LRE represents the less-radiation population. The heatmap of metabolites from the univariate analysis shows that 11 metabolites are downregulated and 15 metabolites are upregulated in the LRE population. The upregulated and downregulated features are shown in red and blue colors, respectively, in Fig. 1.

Through univariate analysis, we ascertained the presence of 29 dysregulated metabolites, demonstrating statistically significant alterations (p-value/False Discovery Rate (FDR) < 0.05) as shown in Figs. 2, 3, 4 and 5.

Among them, 24 metabolites such as 3-Indoxylsulfate, Citrate, 3-hydroxyisovalerate, Ethanol, Taurine, 2-hydroxy isovalerate, Trigonelline, Fumarate, Aconitate, Allantoin, Formate, Acetate, NAC (n-acetyl cysteine), Glycine, Sugar moiety/Glucose, Dimethylglycine, Succinate, Hippurate, IMP (inositol monophosphate), 1-methyl nicotinamide, Galactose, Anserine, SAH (s-adenosylhomocysteine), and 4-HPA (4-hydroxyphenylacetate) resulted from *t*-test analysis. The application of a volcano plot unveiled that those 12 metabolites displayed a Fold Change (FC) exceeding a defined threshold of 2. Our comprehensive fold change analysis identified 20 compounds that exhibited statistically significant differences. Notably, all the metabolites observed in the volcano plot and the fold change analysis were consistent with those observed in the *t*-test. Additionally, two more compounds, namely 2′-deoxyadenosine and methanol, were noted through the fold change analysis. The metabolites from fold change analysis, *t*-test, and volcano plot were listed in Tables 3, 4, and 5, respectively.

The data was normalized and plotted after the univariate analysis, as shown in the Supplementary Fig. 1. Supplementary Fig. 2 shows the correlation illustration of metabolites with the color palette aligned with the correlation intensity. Supplementary Fig. 3 shows the metabolites assigned in 1D ^{1}H NMR spectra.

3.2 Multivariate analysis

We performed multivariate metabolomics analysis of the high radiation-exposed population (HRE) and less radiation-exposed population (LRE) using PCA and PLS-DA analyses to check the data variance.

A permutation test was performed to assess the significance of class discrimination. In each permutation, a PLS-DA model was built between the data (X) and the permuted class labels (Y) using the optimal number of components determined by cross-validation for the model based on the original class assignment. The 2-D Score plot between

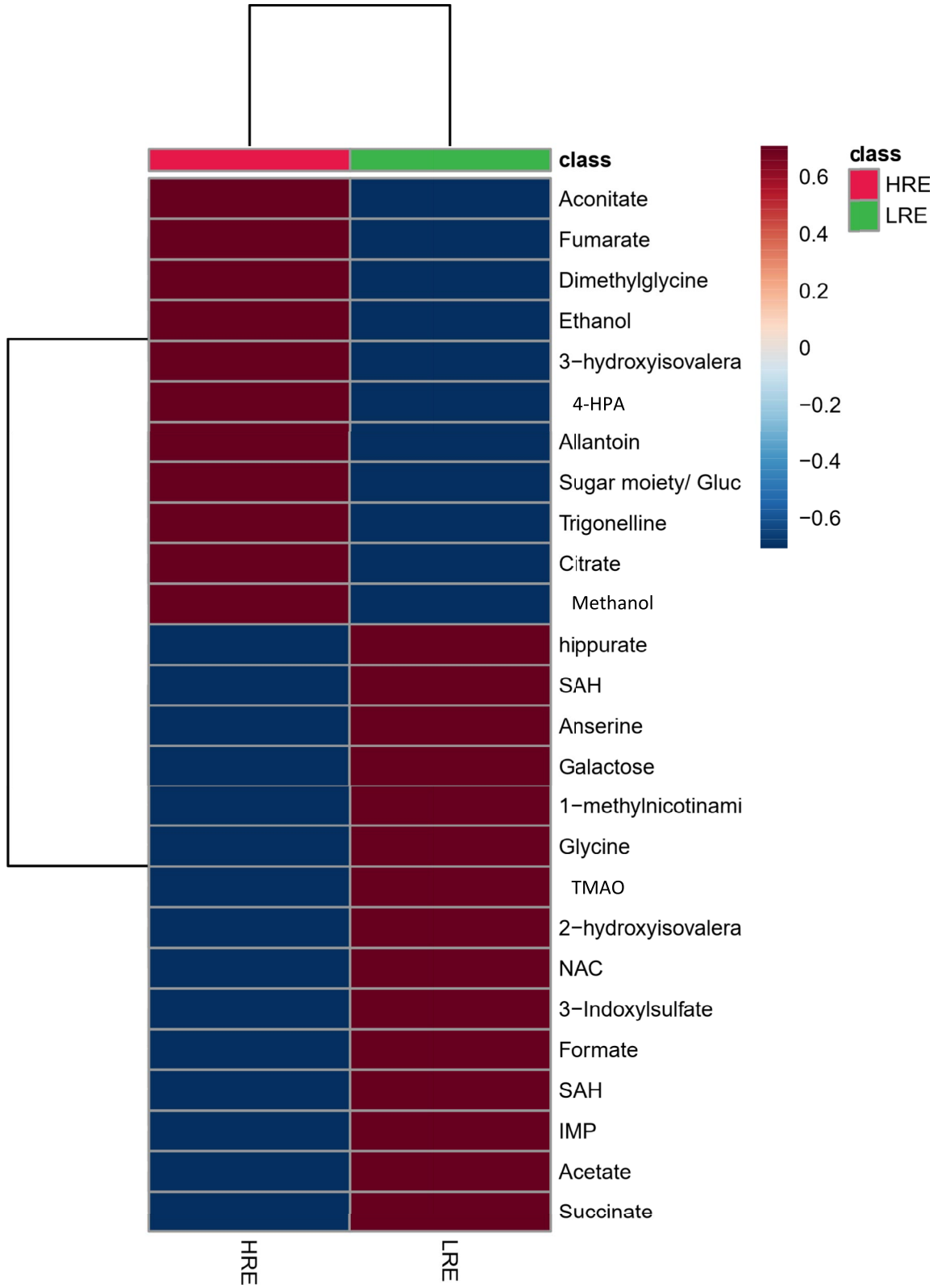


Fig. 1 The Heatmap of metabolites resulted from the univariate analysis. *HRE* high radiation exposed population, *LRE* low radiation exposed population

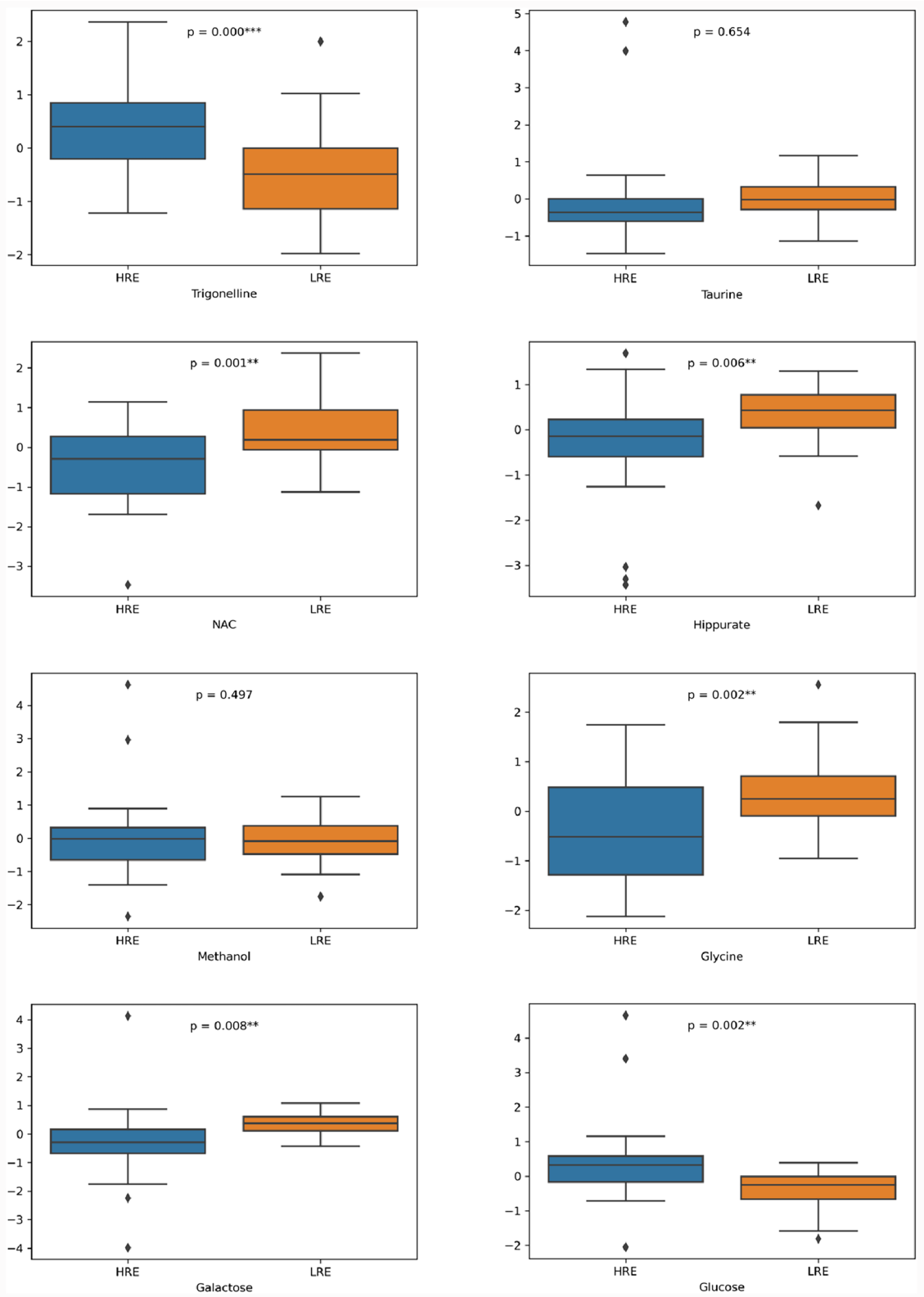


Fig. 2 The univariate analysis of *HRE* high radiation exposure and *LRE* low radiation exposure population results the up and down regulation. The p-value has been mentioned individually

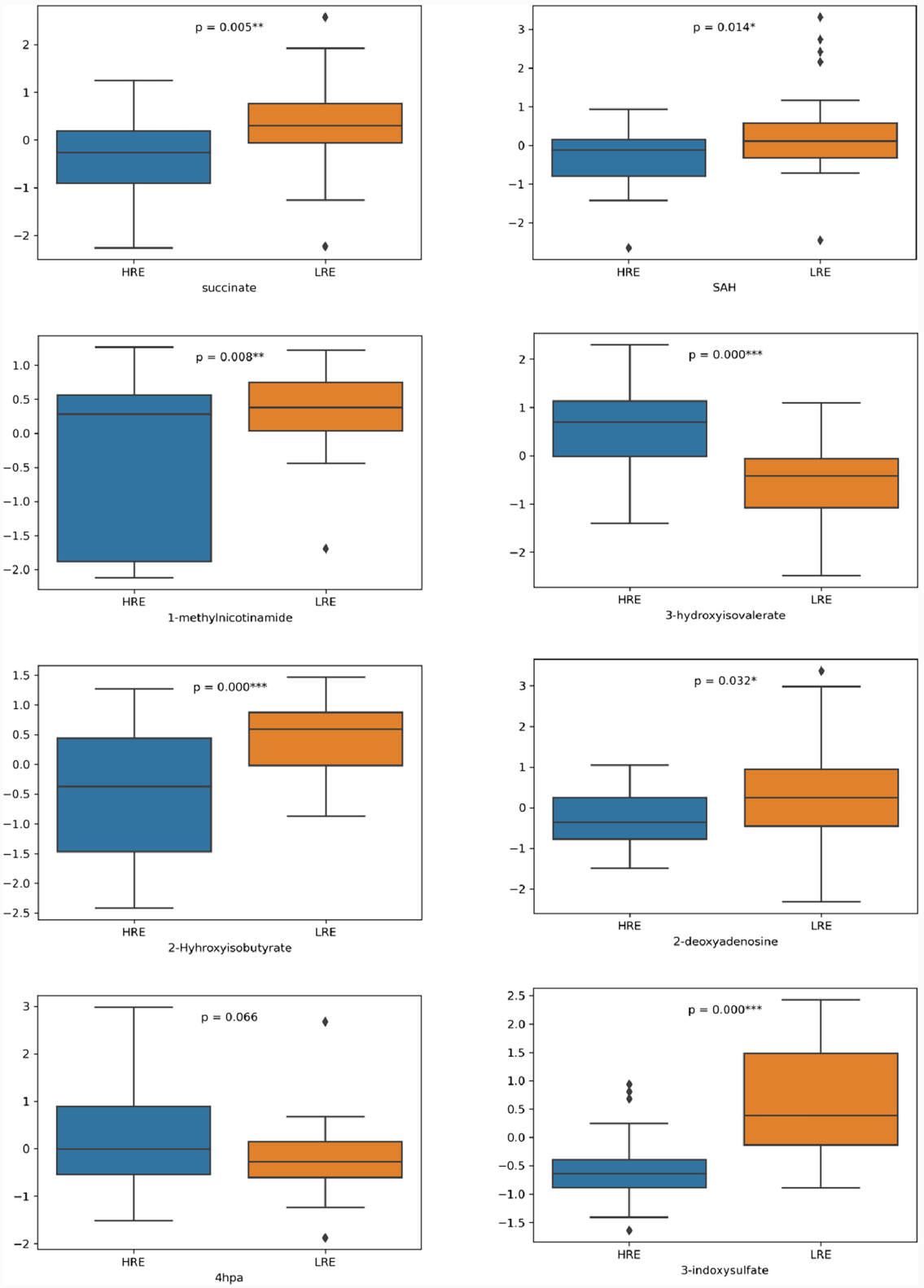


Fig. 3 The univariate analysis of *HRE* high radiation exposure and *LRE* low radiation exposure population results the up and down regulation. The p-value has been mentioned individually

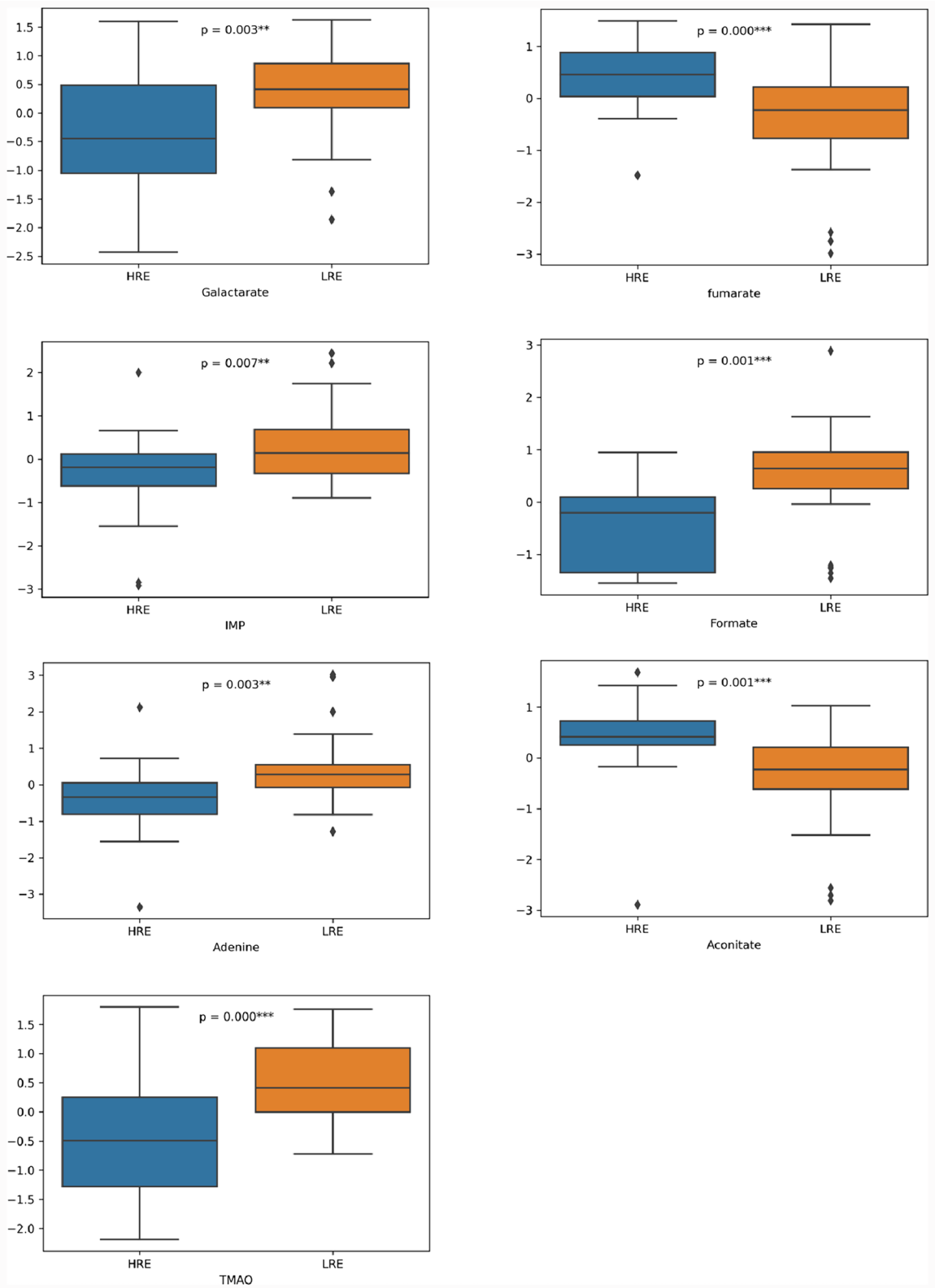


Fig. 4 The univariate analysis of *HRE* high radiation exposure and *LRE* low radiation exposure population results the up and down regulation. The p-value has been mentioned individually

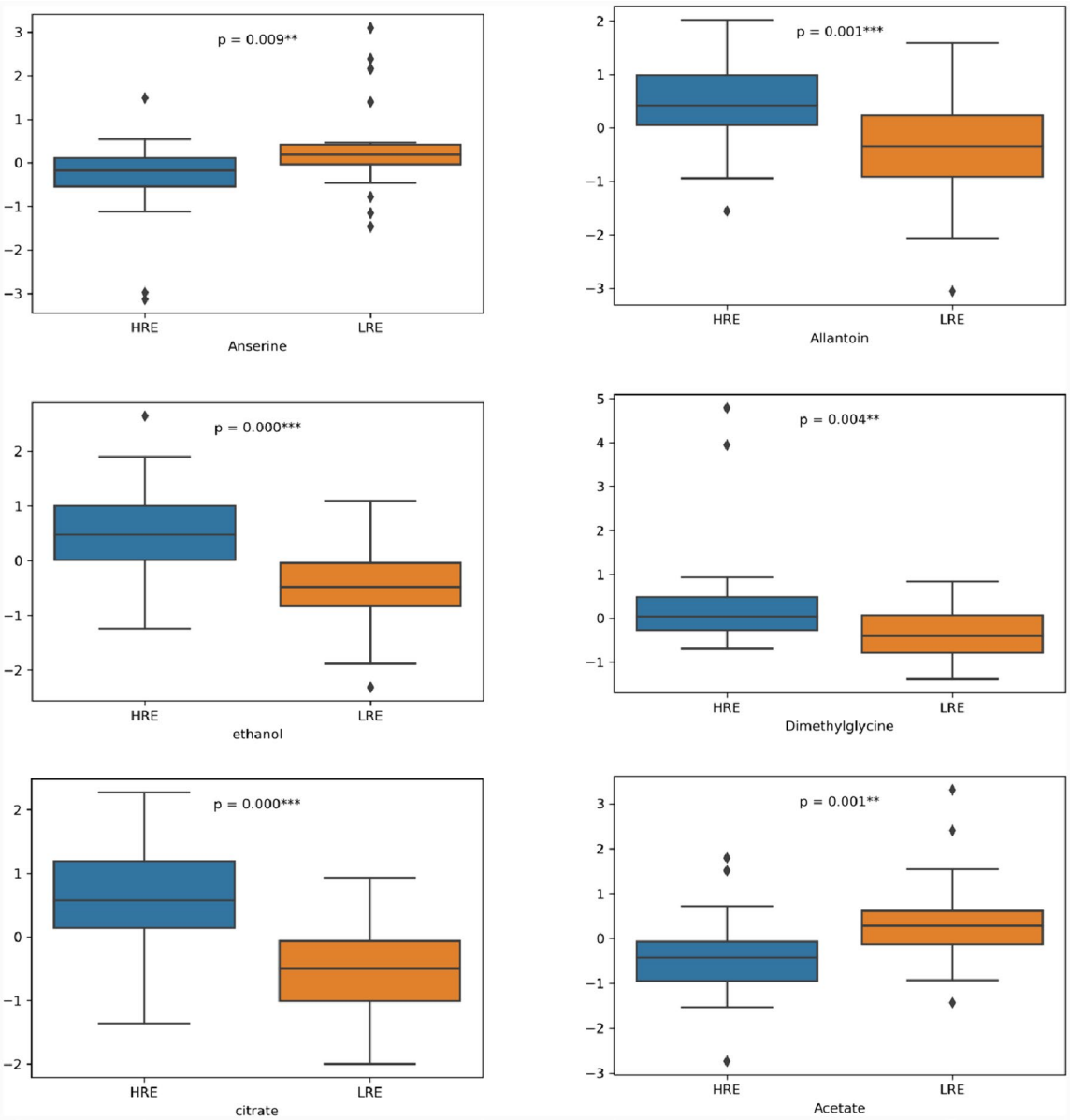


Fig. 5 The univariate analysis of *HRE* high radiation exposure and *LRE* low radiation exposure population results the up and down regulation. The p-value has been mentioned individually

Component 1 and Component 2 is shown in Fig. 6. Each point on the plot represents an observation/sample, and the position of the point in the plot indicates its score on the corresponding latent variables Component 1 and Component 2. The explained variances are shown in the brackets. The samples from the same group are clustered together in the score plot and are well-separated with no overlap, indicating a good discrimination to capture the underlying group differences. The principal components (PC) showed a 23.7% variance in PC 1 and 9.9% in PC 2 (Fig. 6a). PLS-DA analysis performed on data also showed similar results, with 23.6% variance in component 1 and 4.5% in component 2 (Fig. 6b). For taking into account the amount of explained Y-variation in each dimension, Variable Importance in Projection (VIP) was used. VIP Scores were calculated for each component. The VIP scores above the threshold value of 1, which are of greater importance, are shown in Fig. 6c. On validation by permutation tests, we obtained the PLS-DA model with an accuracy of 0.933 ($R^2 = 0.977$ and $Q^2 = 0.709$) and the Orthogonal Projections to Latent Structures Discriminant Analysis (OPLS-DA) model with $R^2Y = 0.955$ and $Q^2 = 0.675$. The permutation of the model set to 100 shows significance with a p-value of 0.01. A model with $R^2 = 0.7$ and $Q^2 = 0.4$ is suitable for biological data. Furthermore,

Table 3 The dysregulated metabolites of HRE and LRE of fold change analysis

Sl. No.	Metabolite	Fold change	log2(FC)
1.	2-deoxyadenosine	0.43556	− 1.1991
2.	4-HPA	3.803	1.9272
3.	Aconitate	2.4822	1.3116
4.	Adenine	0.40978	− 1.2871
5.	Anserine	0.25148	− 1.9915
6.	Citrate	2.1194	1.0837
7.	Dimethylglycine	2.0148	1.0106
8.	Ethanol	2.4685	1.3036
9.	Formate	0.11858	− 3.076
10.	Fumarate	2.6468	1.4042
11.	Glucose	13.032	3.704
12.	Glycine	2.4978	1.3207
13.	Hippurate	3.6702	1.8758
14.	IMP	0.41905	− 1.2548
15.	Methanol	2.0342	1.0244
16.	SAH	0.214	− 2.2243
17.	Taurine	2.4914	1.317
18.	TMAO	2.7807	1.4755
19.	Trigonelline	3.33	1.7355
20.	Adenine	2.9494	1.5604

Table 4 The dysregulated metabolites of HRE and LRE of *t*-test analysis

Sl. No.	Peaks (ppm)	t. stat	p. value	FDR
1.	3-Indoxylsulfate	− 5.5968	6.23E−07	9.93E−06
2.	Citrate	5.5423	7.64E−07	9.93E−06
3.	3-Hydroxyisovalerate	5.1584	3.16E−06	2.74E−05
4.	Ethanol	4.2161	8.81E−05	0.00054229
5.	Taurine	− 4.1663	0.00010429	0.00054229
6.	2-Hydroxyisovalerate	− 4.0301	0.00016449	0.00071278
7.	Trigonelline	3.9238	0.00023355	0.00086747
8.	Fumarate	3.6956	0.00048795	0.0015858
9.	Aconitate	3.5798	0.00070322	0.001944
10.	Allantoin	3.5597	0.00074874	0.001944
11.	Formate	− 3.5296	0.00082246	0.001944
12.	Acetate	− 3.4436	0.0010722	0.002323
13.	NAC	− 3.3473	0.0014371	0.0028742
14.	Glycine	− 3.3014	0.0016501	0.0029654
15.	Sugar moiety/glucose	3.2893	0.0017108	0.0029654
16.	Dimethylglycine	2.9614	0.0044325	0.0072029
17.	Succinate	− 2.8945	0.0053442	0.0081735
18.	Hippurate	− 2.8302	0.0063816	0.0092179
19.	IMP	− 2.8023	0.0068861	0.0094231
20.	1-Methylnicotinamide	− 2.7642	0.0076357	0.0099216
21.	Galactose	− 2.7463	0.0080136	0.0099216
22.	Anserine	− 2.7152	0.0087118	0.010296
23.	SAH	− 2.5433	0.013669	0.015452
24.	4-HPA	1.8724	0.0662	0.068848

Table 5 The dysregulated metabolites of HRE and LRE of volcano plot

Sl. No.	Peaks (ppm)	FC	log2(FC)	p-Value
1.	Ethanol	4.2319	2.0813	8.8127e−05
2.	Glucose	14.77	3.8846	0.0017108
3.	3-Indoxyl sulfate	0.13142	− 2.9277	6.2328e−07
4.	SAH	0.25064	− 1.9963	0.013669
5.	Anserine	0.25925	− 1.9476	0.0087118
6.	Trigonelline	3.3897	1.7612	0.00023355
7.	Aconitate	3.1824	1.6701	0.00070322
8.	Acetate	0.32977	− 1.6005	0.0010722
9.	Allantoin	2.7028	1.4345	0.00074874
10.	Succinate	0.39027	− 1.3575	0.0053442
11.	TMAO	0.39767	− 1.3303	0.00010429
12.	Formate	0.45282	− 1.143	0.0063816

the variables were chosen using the Variable Importance in Projection (VIP) plots with a 0.95 confidence level. This indicates that both models' accuracy was well above this benchmark and is likely helpful for predicting group membership or identifying biomarkers. VIP analyses enabled us to choose relevant features based on biological relevance, statistical significance, or both. 3-Indoxylsulfate, Citrate, 3-hydroxyisovalerate, Ethanol, TMAO, 2-hydroxyisovalerate, Trigonelline, Fumarate, Aconitate, Allantoin, Formate, Acetate, NAC (n-acetyl cysteine), Glycine, and Sugar moiety/ Glucose.

Elevated radiation exposure levels have been associated with the induction of oxidative stress (Wei et al., 2019). One consequence of this increased oxidative stress is the heightened production of mitochondrial reactive oxygen species (ROS) (Islam & Shekhar, 2015). Consequently, a cascade of metabolic changes ensues, potentially leading to the downregulation of certain metabolites. Among these alterations, our investigations revealed upregulation in the intermediate metabolites associated with the sugar moiety (glucose) and the tricarboxylic acid (TCA) cycle, such as citrate and aconitate. Various metabolites have been shown to respond in a compensatory manner in response to oxidative stress. Trigonelline and dimethylglycine, for instance, are known for their antioxidant properties and have been reported to counteract oxidative stress (Chowdhury et al., 2018; Bai et al., 2016). Consequently, in our studies, both trigonelline and dimethylglycine exhibited upregulation, suggesting their roles in mitigating oxidative stress induced by radiation exposure.

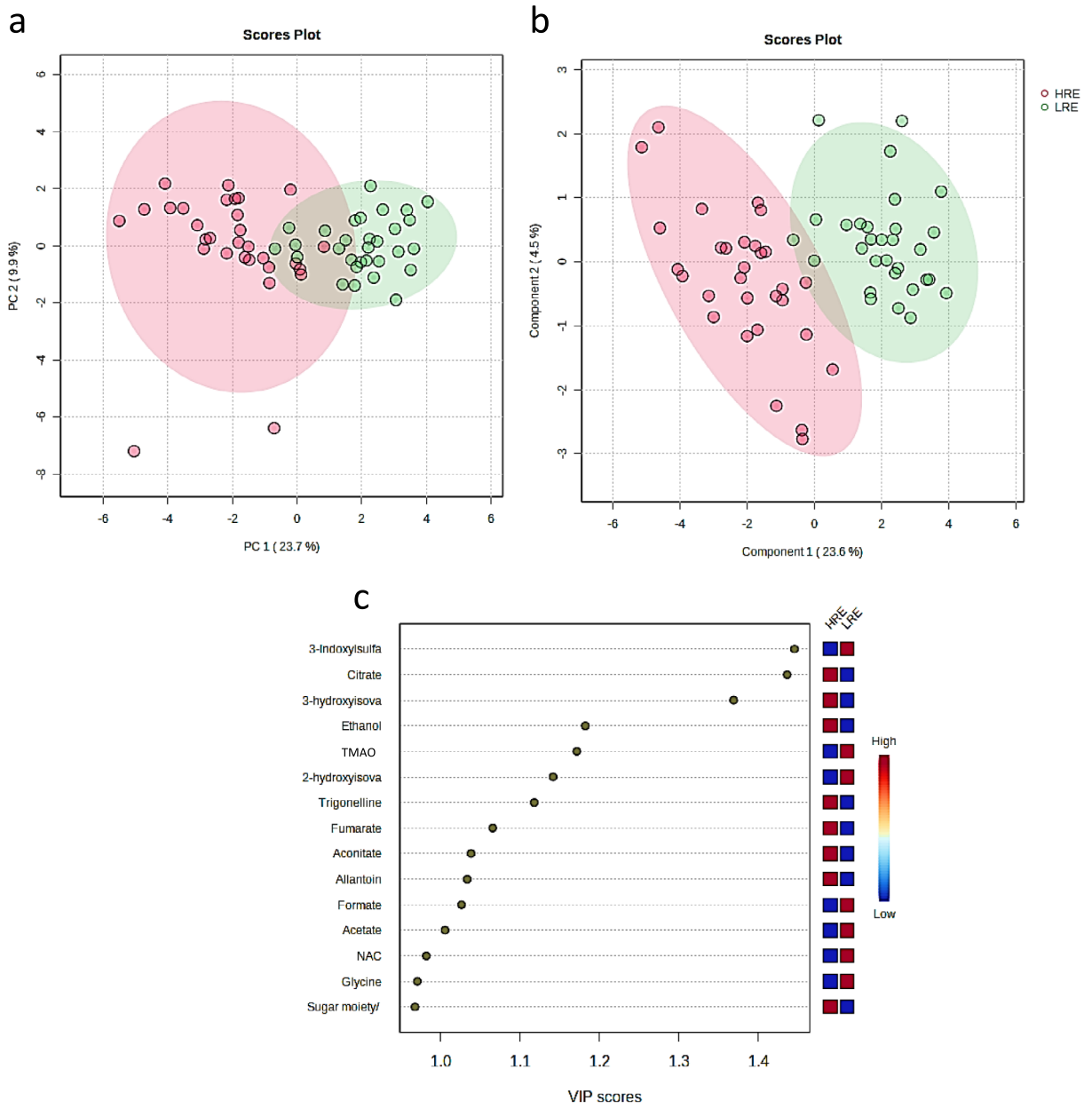


Fig. 6 The important metabolites identified by PLS-DA using VIP score in high radiation population (Group A) and less radiation population (Group B)

Allantoin, derived from the oxidation of uric acid and associated with purine metabolism, acts as an oxidative stress marker and an antioxidant (Kand'ár & Záková, 2008). Our studies demonstrated the upregulation of allantoin in response to radiation exposure. Similarly, 3-Hydroxyisovalerate, a normal human metabolite excreted in urine stemming from the leucine degradation pathway, showed elevated levels—however, the exact significance of these metabolites in the context of radiation exposure warrants further investigation. Taurine, well-recognized for its antioxidant properties (Baliou et al., 2021), exhibited downregulation in our studies. This reduction in taurine levels may potentially compromise the body's ability to effectively counteract oxidative stress. N-acetyl cysteine (NAC), which acts as an indirect antioxidant through promoting glutathione (GSH) biosynthesis (Aldini et al., 2018), was found to be downregulated in our study. Conversely, dimethylglycine, another

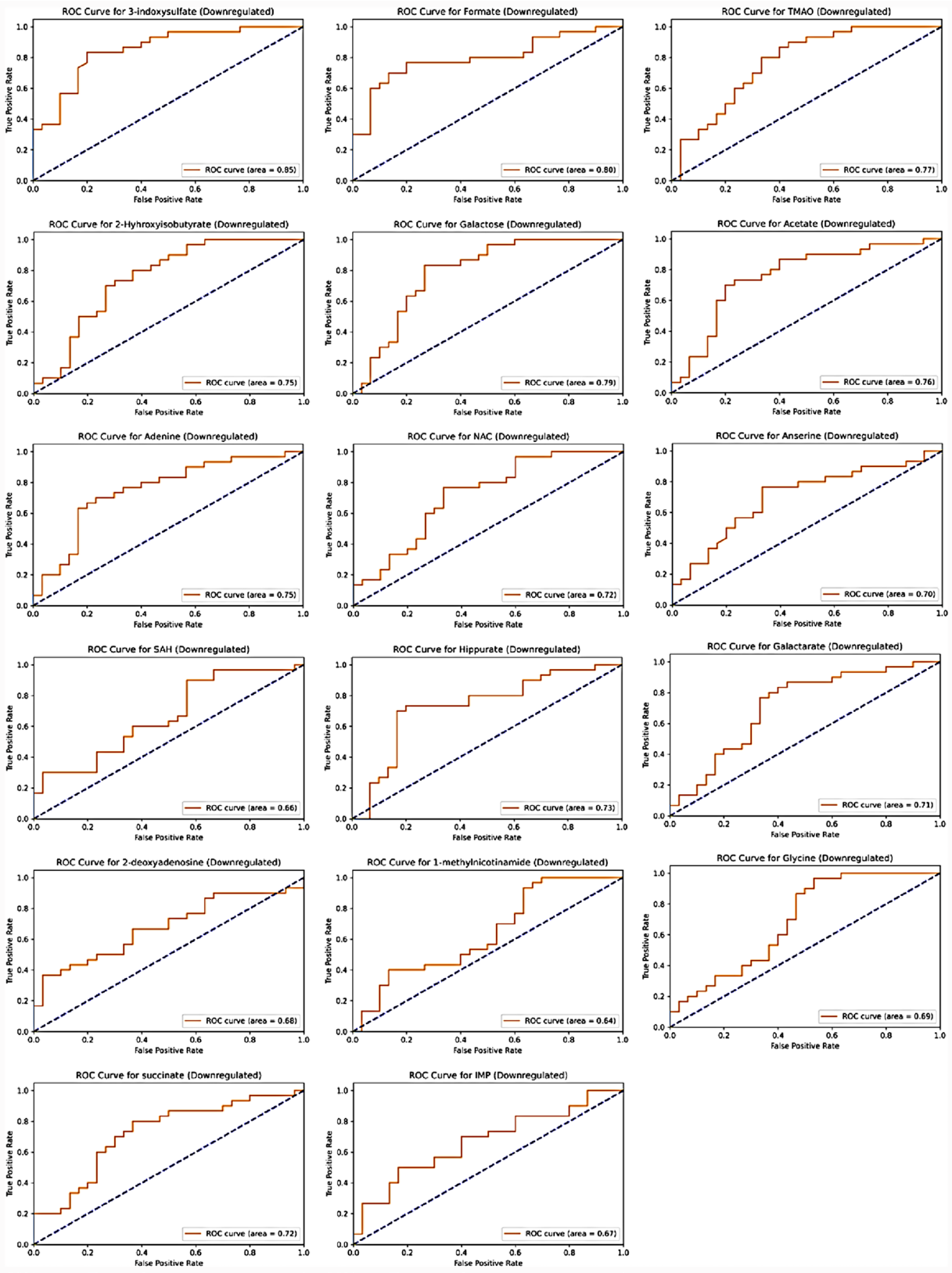


Fig. 7 The metabolites were further validated with ROC—area under the curve (AUC) analysis. More than 0.5 can be considered a discriminative population. If less than 0.5, then non-discriminative

metabolite with reported responses to oxidative stress, displayed upregulation in high radiation populations. The metabolite 4-hydroxyphenyl acetate (4-HPA) potentially possesses antioxidant properties and anti-inflammatory mechanisms, potentially mitigating oxidative stress-related disorders (Zhao et al., 2018).

Acetate, serving as a primary energy source and crucial for the synthesis of fatty acids and cholesterol, may experience decreased levels in response to radiation-induced metabolic shifts (Moffett et al., 2020). Additionally, radiation-induced damage to the gut microbiota, responsible for fermenting dietary fibers into short-chain fatty acids, including acetate, might further contribute to the observed reductions in acetate levels.

Trigonelline, a byproduct of the niacin (vitamin B3) pathway, exhibited alterations in urine excretion, potentially indicative of a distinct niacin metabolism class. In our studies, it was found to be upregulated in the high-radiation population.

Hippurate, produced through the conjugation of benzoic acid with glycine and associated with gut microbial diversity (Brial et al., 2021), was observed to be upregulated in high-radiation populations. While it is associated with increased consumption of phenolic compounds and linked to certain medical conditions, its direct relationship with radiation exposure remains to be fully elucidated. Trimethylamine (TMA) is synthesized within the intestinal tract due to gut microbiota metabolizing dietary components such as carnitine, choline, and choline-containing compounds. This TMA can subsequently be absorbed from the intestinal tract and transported to the liver. Inside the liver, specific enzymes known as flavin-dependent monooxygenase (FMO) isoforms 1 and 3 catalyze the conversion of TMA into trimethylamine N-oxide (TMAO). Notably, our research revealed the downregulation of TMAO in individuals with high radiation exposure (HRE), implying potential disturbances in the gut microbiota composition within this population (Janeiro et al., 2018). Processes involving S-adenosyl methionine (SAM) contribute to the pool of physiological methanol alongside methanol produced by intestinal bacteria and dietary sources. Methanol and S-adenosyl homocysteine may arise from SAM (Dorokhov et al., 2015). In our study, methanol exhibited upregulation in the high-radiation population, while S-adenosyl homocysteine was elevated in the less-radiation-exposed population, emphasizing the potential role of gut microbiota. These findings suggest perturbation or dysbiosis in radiation-exposed humans, warranting further investigation through detailed microbiome studies to comprehend the extent of gut microbiota changes due to high radiation exposure.

The ROC plot shown in Fig. 7 further strengthens the validity of these metabolites. These represented metabolites would be considered potential biomarkers for further screening in a large cohort. The area under the ROC (AUC) above 0.5 is considered a good model score. The 3-indoxyl sulfate shows the highest area of 0.85, which is also considered a good model score. Then the Formate (AUC 0.80), TMAO (AUC 0.77), Acetate (AUC 0.76), Galactose (AUC 0.79), Anserine (AUC 0.70), NAC (AUC 0.72), 2-hydroxyisobutyrate (AUC 0.75), Adenine (AUC 0.75), SAH (AUC 0.66), Hippurate (AUC 0.73), 2-deoxyadenosine (AUC 0.68), 1-methyl nicotinamide (AUC 0.64), IMP (AUC 0.67), Galactarate (AUC 0.71), and Glycine (AUC 0.69). The pathway analysis and their impact score figures are in Supplementary Fig. 3. In particular, Glyoxylate and dicarboxylate and the TCA cycle metabolism pathway have been perturbed with an FDR value of < 0.05. This is the first study of the metabolites in urine samples of humans naturally exposed to these two different microenvironments, aiming to understand short-term metabolic dysregulations.

4 Conclusion

The purpose of this study was to initiate an exploration using urine metabolomics and ^{1}H NMR spectroscopy to identify specific dysregulated metabolites associated with RF-EM radiation exposure. The objective was to pinpoint potential biomarkers for future validation. Based on these preliminary findings, there appears to be a possible connection between RF-EM radiation exposure, oxidative stress, and disruptions in the gut microbiota balance. Nevertheless, it's imperative to stress that additional investigations with a larger and more diverse population are necessary to validate these identified biomarkers and gain a more comprehensive understanding of the effects of RF-EM radiation exposure on human health. Furthermore, individuals with lower levels of radiation exposure exhibited metabolite signatures of a healthier gut microbiota system, indicating a potential association between radiation exposure and microbiota health. However, it is crucial to emphasize that further research is essential for confirmation. Future studies involve conducting a comprehensive study involving individuals with substantial RF-EM radiation exposure alongside a control group of unexposed individuals.

Supplementary Information The online version contains supplementary material available at https://doi.org/10.1007/s11306-024-02121-2.

Acknowledgements We thank the ICGEB New Delhi core funds and Department of Biotechnology (DBT), Government of India, and for the NMR facility at ICGEB, New Delhi, India. AKM is supported by Junior Research Fellowship from the Department of Biotechnology (DBT), Government of India

Author contributions NMR—Designed, performed experiments, reviewed, wrote, and refined the manuscript. AM—performed experiments, analyzed, reviewed, and wrote the manuscript. NK—Collected

& Prepared samples for experiments. Analysed and reviewed the manuscript. SK—Analysed, reviewed, and refined the manuscript. All authors have given consent and approved the final version of the article.

Data availability Raw and processed NMR datasets (time domain data and FT transform processed data) from this study can be retrieved from the online repository at the Indian Metabolome Data Archive (IMDA) of Indian Biological Data Centre (IBDC) with IMDA Project id: IMP_100010. https://ibdc.rcb.res.in/imda/.

Software availability Metaboanalyst (https://www.metaboanalyst.ca/), Chenomx evaluation tool (https://www.chenomx.com/), and SPSS tool (https://www.ibm.com/products/spss-statistics) were used in this study.

Declarations

Conflict of interest Neel Mani Rangesh works with O/o the CGMT, Bihar Telecom Circle, Bharat Sanchar Nigam Limited (BSNL), A Government of India Telecommunication Enterprise. Other authors declare no conflict of interest.

Ethical approval The Institute Ethical Committees (IEC) of Indira Gandhi Institute of Medical Sciences (IGIMS), Patna, reviewed and approved the study vide approval numbers 1145/IEC / IGIMS/2019/16.10.2019. Written and signed informed consent were sought and obtained from all participants. Before obtaining consent, the Patient's Information Sheet (PIS) and Patient's Informed Consent Form (PICF) were explained to the patients and attendants in multilingual English and Hindi.

References

Aldini, G., Altomare, A., Baron, G., Vistoli, G., Carini, M., Borsani, L., & Sergio, F. (2018). N-Acetylcysteine as an antioxidant and disulphide breaking agent: The reasons why. *Free Radical Research, 52*, 751.

Baan, R., Grosse, Y., Lauby-Secretan, B., El Ghissassi, F., Bouvard, V., Benbrahim-Tallaa, L., Guha, N., Islami, F., Galichet, L., & Straif, K. (2011). Carcinogenicity of radiofrequency electromagnetic fields. *The Lancet Oncology, 12*, 624.

Bai, K., Xu, W., Zhang, J., Kou, T., Niu, Y., Wan, X., Zhang, L., Wang, C., & Wang, T. (2016). Assessment of free radical scavenging activity of dimethylglycine sodium salt and its role in providing protection against lipopolysaccharide-induced oxidative stress in mice. *PLoS ONE*. https://doi.org/10.1371/journal.pone.0155393

Baliou, S., Adamaki, M., Ioannou, P., Pappa, A., Panayiotidis, M. I., Spandidos, D. A., Christodoulou, I., Kyriakopoulos, A. M., & Zoumpourlis, V. (2021). rotective role of taurine against oxidative stress. *Molecular Medicine Reports, 24*(2), 605. https://doi.org/10.3892/mmr.2021.12242

Beckonert, O., Keun, H. C., Ebbels, T. M., Bundy, J., Holmes, E., Lindon, J. C., & Nicholson, J. K. (2007). Metabolic profiling, metabolomic and metabonomic procedures for NMR spectroscopy of urine, plasma, serum and tissue extracts. *Nature Protocols, 2*, 2692.

Bollard, M. E., Stanley, E. G., Lindon, J. C., Nicholson, J. K., & Holmes, E. (2005). NMR-based metabonomic approaches for evaluating physiological influences on biofluid composition. *NMR in Biomedicine, 18*, 143.

Brial, F., Chilloux, J., Nielsen, T., Vieira-Silva, S., Falony, G., Andrikopoulos, P., Olanipekun, M., Hoyles, L., Djouadi, F., Neves, A. L., Rodriguez-Martinez, A., Mouawad, G. I., Pons, N., Forslund, S., Le-Chatelier, E., Lay, A. L., Nicholson, J., Hansen, T., Hyötyläinen, T., … Dumas, M. E. (2021). Human and preclinical studies of the host-gut microbiome co-metabolite hippurate as a marker and mediator of metabolic health. *Gut, 70*(11), 2105–2114. https://doi.org/10.1136/gutjnl-2020-323314

Chowdhury, A. A., Gawali, N. B., Munshi, R., & Juvekar, A. R. (2018). Trigonelline insulates against oxidative stress, proinflammatory cytokines and restores BDNF levels in lipopolysaccharide induced cognitive impairment in adult mice. *Metabolic Brain Disease, 33*, 681–691.

Danker-Hopfe, H., Dorn, H., Sauter, C., Schmid, G., & Eggert, T. (2020). An experimental study on effects of radiofrequency electromagnetic fields on sleep in healthy elderly males and females: Gender matters! *Environmental Research*. https://doi.org/10.1016/j.envres.2020.109181

Dorokhov, Y. L., Shindyapina, A. V., Sheshukova, E. V., & Komarova, T. V. (2015). Metabolic methanol: Molecular pathways and physiological roles. *Physiological Reviews, 95*, 603.

Fan, T. W. M., & Lane, A. N. (2016). Applications of NMR spectroscopy to systems biochemistry. *Progress in Nuclear Magnetic Resonance Spectroscopy, 92*, 18.

Gong, Y., Capstick, M. H., Kuehn, S., Wilson, P. F., Ladbury, J. M., Koepke, G., & Kuster, N. (2017). Life-time dosimetric assessment for mice and rats exposed in reverberation chambers for the two-year NTP cancer bioassay study on cell phone radiation. *IEEE Transactions on Electromagnetic Compatibility, 59*(6), 1798–1808.

González-Domínguez, R., González-Domínguez, Á., Sayago, A., & Fernández-Recamales, Á. (2020). Recommendations and best practices for standardizing the pre-analytical processing of blood and urine samples in metabolomics. *Metabolites, 10*(6), 229. https://doi.org/10.3390/metabo10060229

Habauzit, D., Le Quément, C., Zhadobov, M., Martin, C., Aubry, M., Sauleau, R., & Le Dréan, Y. (2014). Transcriptome analysis reveals the contribution of thermal and the specific effects in cellular response to millimeter wave exposure. *PLoS ONE, 9*(10), e109435.

International Agency for Research on Cancer (IARC). (2013). *Monograph non-ionizing radiation part-2 radiofrequency electromagnetic fields*. p. 102.

Islam, M. M. T., & Shekhar, H. U. (2015). Impact of oxidative stress on human health. In V. Rani & U. Yadav (Eds.), *Free radicals in human health and disease*. Springer.

Janeiro, M. H., Ramírez, M. J., Milagro, F. I., Martínez, J. A., & Solas, M. (2018). Implication of trimethylamine N-oxide (TMAO) in disease: Potential biomarker or new therapeutic target. *Nutrients, 10*(10), 1398. https://doi.org/10.3390/nu10101398

Kand'ár, R., & Záková, P. (2008). Allantoin as a marker of oxidative stress in human erythrocytes. *Clinical Chemistry and Laboratory Medicine, 46*(9), 1270–1274. https://doi.org/10.1515/CCLM.2008.244

Lin, J. C. (2019). The significance of primary tumors in the NTP study of chronic rat exposure to cell phone radiation. *IEEE Microwave Magazine, 20*, 18.

Lv, Y. G., & Liu, J. (2003). A theoretical way of distinguishing the thermal and non-thermal effects in biological tissues subject to EM radiation. *Forschung Im Ingenieurwesen, 67*, 242.

Moffett, J. R., Puthillathu, N., Vengilote, R., Jaworski, D. M., & Namboodiri, A. M. (2020). Acetate revisited: a key biomolecule at the nexus of metabolism, epigenetics, and oncogenesis—part 2: Acetate and ACSS2 in health and disease. *Frontiers in Physiology*. https://doi.org/10.3389/fphys.2020.580171

Nicholson, J. K., & Wilson, I. D. (2003). Understanding "global" systems biology: Metabonomics and the continuum of metabolism. *Nature Reviews Drug Discovery, 2*, 668.

Siddiqi, N., & Al Nazwani, N. (2019). Effects of electromagnetic field on the development of chick embryo: An in vivo study. In J. Smith (Ed.), *Electromagnetic fields and waves.* IntechOpen.

Wang, J. C., Lim, E. G., Leach, M., Wang, Z., Man, K. L., & Huang, Y. (2016). Two methods of SAR measurement for wearable electronic devices. In: *Proceedings of the international multi conference of engineers and computer scientists*. Vol. 2.

Wei, J., Wang, B., Wang, H., Meng, L., Zhao, Q., Li, X., Xin, Y., & Jiang, X. (2019). Radiation-induced normal tissue damage: Oxidative stress and epigenetic mechanisms. *Oxidative Medicine and Cellular Longevity*. https://doi.org/10.1155/2019/3010342

Wood, A. W., & Karipidis, K. (2017). *Non-ionizing radiation protection: summary of research and policy options*. Wiley.

Wyde, M., Cesta, M., Blystone, C., Elmore, S., Foster, P., Hooth, M., Bucher, J. (2016). Report of partial findings from the national toxicology program carcinogenesis studies of cell phone radiofrequency radiation in Hsd: Sprague Dawley® SD rats (Whole Body Exposure).

Zhao, H., Jiang, Z., Chang, X., Xue, H., Yahefu, W., & Zhang, X. (2018). 4-Hydroxyphenylacetic acid prevents acute APAP-induced liver injury by increasing phase II and antioxidant enzymes in mice. *Frontiers in Pharmacology*. https://doi.org/10.3389/fphar.2018.00653

Publisher's Note Springer Nature remains neutral with regard to jurisdictional claims in published maps and institutional affiliations.

Springer Nature or its licensor (e.g. a society or other partner) holds exclusive rights to this article under a publishing agreement with the author(s) or other rightsholder(s); author self-archiving of the accepted manuscript version of this article is solely governed by the terms of such publishing agreement and applicable law.